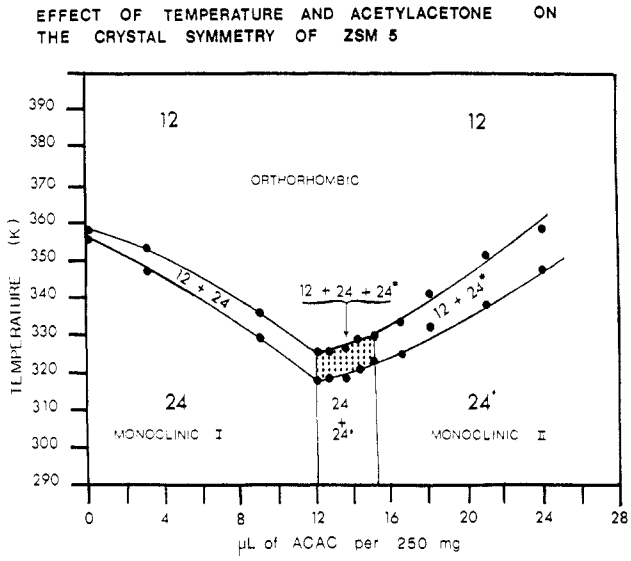

Figure 12. Phase diagram showing the relationship between the three observed phases (monoclinic I, monoclinic II and orthorhombic) with variation of temperature and the concentration of acetylacetone. All three phases coexist in the central region of the diagram.

a greater or lesser degree, the powder diffraction data show the loss of the two reflections at $2\theta \simeq 24.4°$. However, the XRD pattern is an average and reflects mainly the lattice periodicity and may not be sensitive enough to detect that the symmetry of the combination of lattice plus sorbates may be lower than that of the lattice alone. In some other situations involving lattice and site symmetry effects, the high-resolution solid-state NMR spectra have been more sensitive to local symmetry than have diffraction measurements.

What is clear, is that the ZSM-5 lattice structure undergoes changes to accommodate sorbed organic molecules and that the details of the change reflect both the nature and the concentration of the sorbed organics at a given temperature. Using the "phase diagrams" of Figures 8 and 12 as guides, we have initiated structural studies of the various unloaded and loaded forms of this zeolite lattice at selected temperatures. The use of synchrotron-based X-radiation should not only provide data of sufficient accuracy to detail the changes in lattice structures, known from preliminary experiments to involve relatively small changes in cell dimensions and angles, but should also allow the prefered sites which the organics occupy within the unit cell to be determined. From these complementary techniques, it is anticipated that a full understanding of this phenomenon at the molecular level will emerge. It should be noted that these effects are by no means universal. The only other zeolite system in which we have observed them to date is the closely related ZSM-11, and they may possibly be related to the very versatile nature of ZSM-5 as a catalyst.

Acknowledgment. The authors acknowledge the financial support of the Natural Sciences and Engineering Research Council of Canada in the form of an Operating Grant (CAF) and Graduate Scholarships (H.S. and G.J.K.). They also acknowledge the Alexander von Humboldt Senior Scientist Award (G.T.K.).

Registry No. *p*-Xylene, 106-42-3; acetylacetone, 123-54-6; pyridine, 110-86-1; dimethyl sulfoxide, 67-68-5; toluene, 108-88-3; benzene, 71-43-2.

Intermolecular Hydrogen-Bonding Effect on ^{13}C NMR Chemical Shifts of Glycine Residue Carbonyl Carbons of Peptides in the Solid State

Shinji Ando,[†] Isao Ando,*[†] Akira Shoji,[‡] and Takuo Ozaki[‡]

Contribution from the Department of Polymer Chemistry, Tokyo Institute of Technology, Ookayama, Meguro-ku, Tokyo, Japan 152, and Department of Industrial Chemistry, College of Technology, Gunma University, Tenjin-cho, Kiryu-shi, Gunma, Japan 376.
Received August 6, 1987

Abstract: In order to investigate the effect of hydrogen bonding on the ^{13}C NMR chemical shifts of carbonyl carbons in peptides in the solid state, ^{13}C CP/MAS NMR spectra were measured for a series of the oligopeptides containing glycine residues, of which the crystal structures were already determined by X-ray diffractions. It was found that the ^{13}C chemical shifts of the carbonyl carbons in the >C=O···H—N< type hydrogen bond form move downfield with a decrease in the hydrogen bond length but those in the >C=O···H—N^+< type hydrogen bond form move upfield with a decrease in the hydrogen bond length. Further, the ^{13}C chemical shift behavior of the carbonyl carbon of polyglycine with forms I and II was reasonably explained in terms of the difference in their hydrogen bond lengths. The quantum chemical calculation of the ^{13}C shielding constant for the model compounds was done and reproduced reasonably the experimental results taking into account the hydrogen bond and conformational effects.

Most recently, we have reported that the isotropic ^{13}C chemical shifts (σ_{iso}) and the principal values of ^{13}C chemical shift tensors (σ_{11}, σ_{22} and σ_{33}) for carbonyl carbon of the glycine residues (Gly CO) incorporated into some homopolypeptide chains such as poly(L-alanine), poly(β-benzyl-L-aspartate), etc., are significantly displaced depending on their conformational changes, as determined by the cross polarization–magic angle spinning (CP–MAS) technique.[1] It is also noted that the magnitude of the chemical shift tensor displacement is larger for σ_{22} (the midfield component) and σ_{33} (the upfield component) than σ_{iso}. The fact that the direction of the conformation-sensitive component σ_{22} is the same as that of the C=O bond suggests that the signal position of Gly

[†] Tokyo Institute of Technology.
[‡] Gunma University.

(1) Ando, S.; Yamanobe, T.; Ando, I.; Shoji, A.; Ozaki, T.; Tabeta, R.; Saitô, H. *J. Am. Chem. Soc.* **1985**, *107*, 7648.

0002-7863/88/1510-3380$01.50/0

CO is closely related to the manner of the hydrogen bond which is formed between amide groups. In addition, the ^{13}C isotropic chemical shift and σ_{22} component of the carbonyl carbon in polyglycine form II ($(Gly)_n$ II; 3_1-helical form) were displaced downfield by 3.3 and 5 ppm, respectively , relative to those of form I ($(Gly)_n$ I; β-antiparallel form). In practice, a strong hydrogen bond is formed in form II, as is evident from the fact that the N···O hydrogen bond length is as long as 2.73 Å in $(Gly)_n$ II[2,3] compared with 2.95 Å in $(Gly)_n$ I.[4] From these, it is expected that the Gly CO ^{13}C chemical shift displacement is related to the hydrogen bond length.

It is well-known that the hydrogen bond plays an important role in forming the stable conformations of polypeptides and proteins. Thus, the nature of the hydrogen bond has been widely studied by various spectroscopic methods. Also, NMR has been used as one of the most powerful tools for obtaining useful information about the details of the hydrogen bond. The ^{13}C NMR chemical shift of the carbonyl carbon is thought to be the most sensitive to the spatial arrangement of the nuclei comprising the hydrogen bond, since the electronic structure of the carbonyl carbon is greatly affected by the hydrogen bond. In fact, it was reported that the formation of the hydrogen bond causes a downfield shift on the carbonyl carbon of peptides in the solution state.[5-9] It is, however, difficult to estimate the hydrogen bond effect on the ^{13}C chemical shift because the observed chemical shifts of the peptides are often the averaged values for all the rotational isomers owing to an interconversion by rapid rotation in the solution state. Therefore, chemical shifts in the solid state provide useful information about the hydrogen bond of the peptides with a fixed conformation. Nevertheless, no attempts have been made to correlate the manner of the hdyrogen bond and ^{13}C chemical shifts of peptide carbonyl carbons in the solid state.

Therefore, the main purpose of the present work is to measure ^{13}C chemical shifts of the glycine carbonyl carbons in peptides containing the glycine residues in the solid state, of which the hydrogen bond lengths and the conformations are determined from X-ray studies. On the basis of these results, the relationship between the ^{13}C chemical shift and the hydrogen bond length will be discussed. In this study, we chose peptides whose Gly CO in the amide group is involved in the intermolecular >C=O···H—N< hydrogen bonds (Gly CO is not in the terminal carboxyl group). These hydrogen bonds are not so bent, and Gly CO participates in only one hydrogen bond, that is, the so-called "two centered hydrogen bond".[10] In order to clarify the origin of the relationship between the ^{13}C chemical shift and the manner of the hydrogen bond, much more profound knowledge of the peptides is required. For this purpose, we attempt to calculate the ^{13}C shielding constants and tensor components of the glycine carbonyl carbons by employing the quantum chemical method.

Experimental Section

Materials. A series of oligopeptides containing glycine residues, except for chloroacetylglycylglycine (ClAc-Gly-Gly), sarcosylglycylglycine (Sar-Gly-Gly), and glycyl-L-phenylalanylglycine (Gly-L-Phe-Gly), were purchased from SIGMA and recrystallized according to the same procedures as those in the X-ray diffraction studies on them.

ClAc-Gly-Gly was synthesized from glycylglycine (Gly-Gly) by chloroacetylation in 1 N NaOH aqueous solution at room temperature with chroloacetyl chloride.[11] Sar-Gly-Gly and Gly-L-Phe-Gly were synthesized according to a fragment condensation of *N*-hydroxysuccinimide esters and amino acids.[12] The N-terminal of the active ester was protected by the *o*-nitrophenylsulfenyl (Nps-) group for avoiding the racemization in the course of the coupling with amino acids. These samples were purified and recrystallized from aqueous solutions. Glycylglycine nitrate (Gly-Gly·HNO_3) was obtained by slow evaporation from a equimolar mixture of glycylgycine and nitric acid in water. Glycyl-L-phenylalanine *p*-toluensulfonate (Gly-L-Phe·TsOH) was crystallized by the vapor diffusion method with ethyl acetate as precipitant. All the samples prepared in this study take the >C=O···H—N type intermolecular hydrogen bonds in the crystalline state.

The polycrystalline samples thus obtained were ground by agate mortar before the NMR measurements were taken to eliminate the orientation anisotropoy of crystals in the spinning rotor.

^{13}C CP-MAS NMR Measurement. ^{13}C CP-MAS NMR spectra were recorded at room temperature with a JEOL GX-270 NMR spectrometer at 67.80 MHz and with a Bruker MSL-400 NMR spectrometer at 100.63 MHz equipped with a CP-MAS accessory. The pulse sequence of the TOSS (total suppresion of side bands) method was also used to avoid the overlap of spinning side bands and intrinsic signals. Field strengths of ^1H decoupling were 1.2 and 1.5 mT, contact times were 2 and 1 ms, repetition times were 5 and 4s, and spectral widths were 27.0 and 31.3 kHz for the GX-270 and MSL-400 spectrometers, respectively. Data points were 8K. Samples were placed in a bullet-type rotor for the GX-270 spectrometer and in a cylindrical rotor for the MSL-400 spectrometer and spun at 3–4 kHz. Spectra were accumulated 100–500 times to achieve a reasonable signal-to-noise ratio. ^{13}C chemical shifts were calibrated indirectly through the adamantane peak observed at upperfield (29.5 ppm relative to tetramethylsilane ($(CH_3)_4Si$)).

Theoretical Calculation. We employed the finite perturbation theory (FPT)[13-15] within the INDO framework for calculating the ^{13}C shielding constant. The FPT INDO theory has an advantage in permitting the calculation of the paramagnetic term without the explicit wave functions of excited states and the one-electron excitation energies, which are hardly obtained in high accuracy by the usual semiempirical MO approximations. This approach reproduces reasonably the experimental ^{13}C chemical shifts of the L-alanine residue in peptides.[16] According to the FPT INDO framework,[13-15] $\sigma^d_{\alpha\beta}(A)$ (diamagnetic term) and $\sigma^p_{\alpha\beta}(A)$ (paramagnetic term) are expressed by

$$\sigma^d_{\alpha\beta} = \frac{e^2}{2mc^2}\sum_\mu\sum_\nu P_{\mu\nu}(0)\left\langle \chi_\mu \left| \frac{(\gamma_\nu\gamma_A\delta_{\alpha\beta} - r_{\nu A}r_{A\beta})}{|\gamma_A|^3} \right| \chi_\nu \right\rangle$$

$$\sigma^p_{\alpha\beta} = -\frac{eh}{mc}i\sum_\mu\sum_\nu \left(\frac{\partial P_{\mu\nu}(H_\alpha)}{\partial H_\alpha} \right)_{H=0} \left\langle \chi_\mu \left| \frac{(\gamma_A \times \nabla)_\beta}{|\gamma_A|^3} \right| \chi_\nu \right\rangle$$

$$\alpha, \beta = x, y, z$$

where the gauge origin of the vector potential is set at the position of nucleus A. The vectors γ_ν and γ_A are the position vectors of the electron considered from a nucleus of the atom containing the atomic orbital (AO) χ_ν and from the nucleus A, respectively. $P_{\mu\nu}(H)$ and $P_{\mu\nu}(0)$ are the elements of the density matrix with and without the perturbation due to the magnetic field, H, respectively.

The ^{13}C shielding constant calculation was carried out by a similar procedure as reported previously.[16] However, the contributions from AOs centered on two different nuclei are not involved. In the calculation, we adopted *N*-acetyl-*N'*-methylglycine amide as a model molecule having the same skeletal bonds as peptides. Formamide and protonated methylamine molecules were then approached with this model to examine the two types of hydrogen bond effects as shown in Figure 4, parts a and b. The bond lengths and bond angles proposed by Momany et al.[17] were

(2) Crick, F. H. C.; Rich, A. *Nature (London)* **1955**, *176*, 780.
(3) Ramachandran, G. N.; Sasisekharan, V.; Ramakrishnan, C. *Biochim. Biophys. Acta* **1966**, *112*, 168.
(4) Lotz, B. *J. Mol. Biol.* **1974**, *87*, 169.
(5) Urry, D. W.; Michell, L. W.; Ohnishi, T. *Proc. Natl. Acad. Sic. U.S.A.* **1974**, *71*, 3265.
(6) Bartman, B.; Debar, C. M.; Blout, E. R. *J. Am. Chem. Soc.* **1977**, *99*, 1028.
(7) London, R. E.; Stewart, J. M.; Cann, J. R.; Matwiyoff, N. A. *Biochemistry* **1978**, *17*, 2271.
(8) Asakura, T.; Kamio, M.; Nishioka, A. *Biopolymers* **1979**, *18*, 467.
(9) Khaled, M. A.; Sugano, H.; Urray, D. A. *Biochim. Biophys. Acta* **1979**, *577*, 273.
(10) (a) Taylor, R.; Kennard, O.; Versichel, W. *J. Am. Chem. Soc.* **1983**, *105*, 5761. (b) Taylor, R.; Kennard, O.; Versichel, W. *J. Am. Chem. Soc.* **1984**, *106*, 244. (c) Taylor, R.; Kennard, O.; Versichel, W. *Acta Crystallogr.* **1984**, *B40*, 280.
(11) Fisher, E. *Chem. Ber.* **1904**, *37*, 2486.
(12) (a) Zervas, L.; Borovas, D.; Gazis, E. *J. Am. Chem. Soc.* **1963**, *85*, 3660. (b) Wünsch, E. *Synthese von Peptiden*; Georg thieme Verlag: Stuttgart, 1974; Teil I and II. (c) Izumiya, N.; Kato, T.; Ohno, M.; Aoygai, H. *Peptide Synthesis*; Maruzen: Tokyo, 1975.
(13) Ditchfield, R.; Miller, D. P.; Pople, J. A. *J. Chem. Phys.* **1971**, *54*, 4186.
(14) Ellis, P. D.; Maciel, G. E.; McIver, J. M., Jr. *J. Am. Chem. Soc.* **1972**, *94*, 4069.
(15) (a) Kondo, M.; Ando, I.; Chûjô, R.; Nishioka, A. *J. Magn. Reson.* **1976**, *24*, 315. (b) Ando, I.; Webb, G. A. *Theory of NMR Parameters*; Academic: London, 1983.
(16) Ando, I.; Saitô, H.; Tabeta, R.; Shoji, A.; Ozaki, T. *Macromolecules* **1984**, *17*, 457.
(17) Momany, F. A.; McGuire, R. F.; Yan, J. F.; Scheraga, H. A. *J. Phys. Chem.* **1971**, *75*, 2286.

Table I. ^{13}C NMR Chemical Shifts of Glycine Residue Carbonyl Carbons for Oligopeptides Containing Glycine Residues As Determined by ^{13}C CP-MAS NMR (±0.2 ppm from TMS) and Their Geometrical Parameters

		geometrical parameters							
			H bond length/Å		H bond angle/deg		dihedral angle[d]/deg		
sample[a]	type[b]	^{13}C chemical shift, δ/ppm	N··O	H··O	C=O··N	N—H··O	φ	ψ	ref
$(Gly^*)_n$ II	1	172.8[c]	2.73	1.84	158.6	146.2	−78.0	145.8	3
Gly-Gly*-L-Val	1	171.1	2.78	1.72	138.3	173.7	−77.1	−22.3	19
ClAc-Gly*-Gly	1	170.5	2.82	2.13	160.2	147.4	−74.5	154.1	20
L-Pro-Gly*-Gly	1	170.0	2.84	2.21	157.0	151.9	−71.3	167.1	21
L-Ala-Gly*-Gly	1	170.2	2.93	2.09	152.3	165.8	−83.2	169.4	22
$(Gly^*)_n$ I	1	169.5[c]	2.95	2.16	149.2	132.8	146.5	−149.9	4
Gly*-Gly	1	168.5	2.97		157.2			152.8	23
Gly*-L-Phe-Gly	1	168.1	3.00	2.21	161.8	163.7		127.6	24
Gly*-DL-Thr	1	167.8	3.02	2.11	161.2	157.8		−175.0	25
Gly*-L-Thr·$2H_2O$	1	168.3	3.05		147.4			−168.7	26
L-Val-Gly*-Gly	1	169.1	3.05	2.19	156.6	152.4	−155.1	154.7	27
Sar-Gly*-Gly	1	168.6	3.06	2.23	135.0	167.1	72.1	−17.4	28
Gly*-Gly·HNO_3	1	166.5	3.12	2.38	161.8	164.6		148.9	29
DL-Leu-Gly*-Gly	2	167.0	2.74		170.5		−167.5	−172.3	30
Gly*-DL-Phe	2	167.5	2.83	2.28	172.8	115.3		−160.3	31
Gly*-L-Phe·HCl·H_2O	2	168.4	2.83	1.93	161.7	152.8		−162.2	32
Gly*-Phe·TsOH	2	169.8	2.92		139.5			−179.0	33
Gly*-Gly-Val	2	170.9	2.99	2.62	109.9	100.9		−155.8	19

[a] The asterisk indicates the glycine residue whose carbonyl carbon was measured. [b] The manner of hydrogen bond. See text. [c] Reference 1. Converted to the present tetramethylsilane reference by adding 1 ppm. [d] For glycine residue.

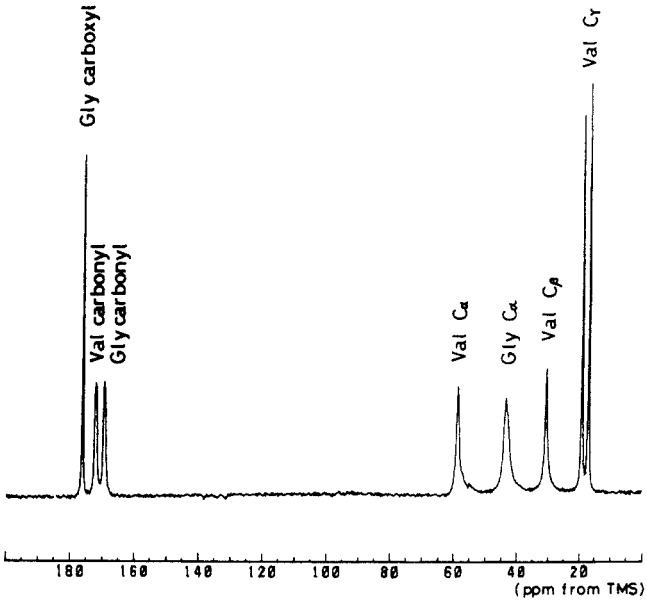

Figure 1. ^{13}C CP-MAS (100.63 MHz) NMR spectrum of L-valylglycylglycine.

used. The calculation was performed as a function of hydrogen bond length (the distance between nitrogen and oxygen atoms, abbreviated as $R_{N\cdots O}$) with the same dihedral angles for the skeletal bonds as those of $(Gly)_n$ I and $(Gly)_n$ II.

A HITAC M280H computer at the Computer Center of the Tokyo Institute of Technology and a HITAC M200H computer at the Computer Center of the Institute for Molecular Science, Okazaki, were used for the calculation.

Results and Discussion

^{13}C NMR Chemical Shifts of the Glycine Carbonyl Carbons in Peptides. A 100.63 MHz ^{13}C CP-MAS NMR spectrum of valylglycylglycine (Val-Gly-Gly) using the TOSS pulse technique is shown as a typical example in Figure 1. ^{13}C CP-MAS spectra of the other remaining samples were also obtained with similar resolutions (figures not shown). Each Gly CO signal can be straightforwardly assigned, because it is resonated upperfield compared with those of the carbonyl carbons of other amino acid residues.[18] This upperfield shift arises from the absence of the

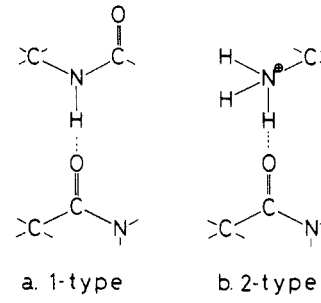

Figure 2. Schematic representations for the two types of hydrogen bonds: (a) 1-type and (b) 2-type.

C_β carbon in the Gly residue. The carbonyl carbon of the C-terminal carboxylic group is resonated downfield by several ppm as a rather sharp peak relative to the internal amide carbonyl carbon. The isotropic ^{13}C chemical shifts of Gly CO carbons determined for all the peptides measured from ^{13}C CP-MAS spectra are listed in Table I, together with the geometrical parameters obtained by X-ray diffraction studies. ^{13}C chemical shifts of the Gly COs in $(Gly)_n$ I and II reported previously[1] are also listed therein. Some of the geometrical parameters were calculated by using the unit cell parameters and fractional coordinates in the literature.

(18) Howarth, O. W. *Prog. NMR Spectrosc.* **1978**, *12*, 1.
(19) Lalitha, V.; Subramanian, E.; Border, J. *Int. J. Peptide Protein Res.* **1984**, *24*, 437.
(20) Rao, S. T. *Cryst. Struct. Commun.* **1973**, *2*, 257.
(21) Lathitha, V.; Subramanian, E.; Parthasarathy, R. *Int. J. Peptide Protein Res.* **1986**, *27*, 223.
(22) Lalitha, V.; Subramanian, E. *Indian J. Pure Appl. Phys.* **1985**, *23*, 506.
(23) Biswas, A. B.; Hughes, E. D.; Sharma, B. D.; Wilson, J. N. *Acta Crystallogr.* **1968**, *B24*, 40.
(24) Marsh, R. E.; Glusker, J. P. *Acta Crystallogr.* **1961**, *14*, 1110.
(25) Swaminathan, P. *Acta Crystallogr.* **1975**, *B31*, 1608.
(26) Yadava, V. S.; Padmanabhan, V. M. *Acta Crystallogr.* **1973**, *B29*, 854.
(27) Lalitha, V.; Murali, R.; Subramanian, E. *Int. J. Peptide Protein Res.* **1986**, *27*, 472.
(28) Glusker, J. P.; Carrel, H. L.; Berman, M.; Gallen, B.; Peck, R. M. *J. Am. Chem. Soc.* **1977**, *99*, 595.
(29) Rao, S. N.; Parthasarathy, R. *Acta Crystallogr.* **1973**, *B29*, 2379.
(30) Goswami, K. N.; Yadava, V. S.; Padmanabhan, V. M. *Acta Crystallogr.* **1977**, *B33*, 1280.
(31) Marsh, R. E. *Acta Crystallogr.* **1976**, *B32*, 66.
(32) Cotrait, P. M.; Barrans, Y. *Acta Crystallogr.* **1974**, *B30*, 1018.
(33) VanDerVeen, J. M.; Low, B. W. *Acta Crystallogr.* **1972**, *B28*, 3548.

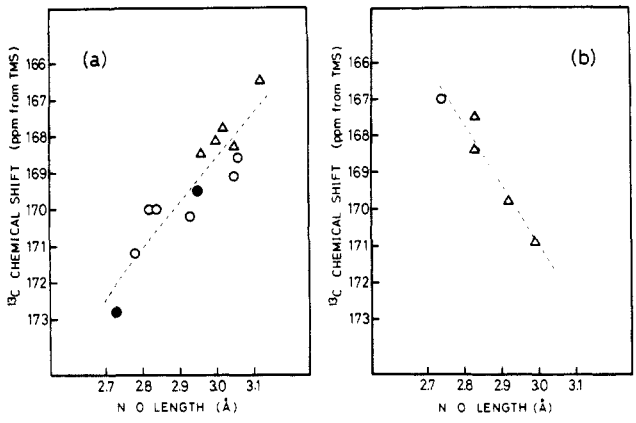

Figure 3. Plots of the observed ^{13}C chemical shifts in the solid state against the N···O hydrogen bond length ($R_{N\cdots O}$) for the 1-type (a) and the 2-type (b) hydrogen bonds. Triangles, open circles, and full circles denote Gly CO of the N-terminal glycyl residues, Gly CO of the second glycyl residues, and Gly CO of polyglycine, respectively.

Figure 2, a and b, shows schematic representations of the two types of hydrogen bonds which exist in peptides considered here as classified by the nature of the proton-donating nitrogen atom. One is denoted as the 1-type hydrogen bond which is formed between amide >C=O and amide >N—H. The other is denoted as the 2-type hydrogen bond which is formed between amide >C=O and N-terminal $-NH_3^+$. The 2-type hydrogen bond exists only in oligopeptides with free end-groups, since such a peptide usually exists as a zwitterion in the crystalline state, where the N-terminal is protonated as NH_3^+ and the C-terminal is deprotonated as COO^-.

Figure 3, a and b, shows the plot of ^{13}C chemical shifts of Gly CO against the N···O hydrogen bond length ($R_{N\cdots O}$) in the 1-type and 2-type hydrogen bonds, respectively. The hydrogen bond effect on the ^{13}C isotropic chemical shift is entirely different between the two types of hydrogen bonds.

In the 1-type, a decrease of $R_{N\cdots O}$ causes a downfield shift. There exists approximately a linear relationship between $R_{N\cdots O}$ and the ^{13}C chemical shifts. It is noted that not only in oligopeptides (dimer or trimer) but also in polypeptides ($(Gly)_n$ I and II) the Gly CO chemical shifts give a similar hydrogen bond dependence. This suggests that the ^{13}C chemical shift of any Gly CO forming the 1-type hydrogen bond is predominantly determined by the manner of hydrogen bond. As is evident from C=O···N and N—H···O angles, most of the 1-type hydrogen bonds are neither so bent nor entirely straight, where a preferred direction of the hydrogen bond approaches the direction of the oxygen atom sp^2 lone pair. The mean value of the C=O···N angles is 153°. This value is slightly larger than that of 120–130° obtained by averaging over the angles for N—H···O=C type hydrogen bonds in 1357 peptides,[10] but the angles of peptides considered here distribute with small discrepancy. Therefore, it can be expected that the "length effect" on the ^{13}C chemical shift in the 1-type hydrogen bond is larger than the "direction effect". Further, the carbonyl carbons of N-terminal glycine residues (indicated by triangles) are resonated upperfield from those of the inner gycine residues (the second residue and polypeptide are indicated by open and full circles, respectively). This may be due to the difference of hydrogen bond length rather than the sequence effect of amino acids.

This result is similar to that by Imashiro et al.[34] that the formation of intra- and intermolecular >C=O···H—O– type hydrogen bonds of hydroxybenzaldehydes in the solid state results in a downfield displacement of ^{13}C chemical hifts of the carbonyl carbon with varying the O···O hydrogen bond length. Similarly, Berglund and Vaughan[35] pointed out a similar correlation between the isotropic ^1H chemical shift and O···O hydrogen bond distance.

(34) Imashiro, F.; Maeda, S.; Takegoshi, K.; Terao, T.; Saika, A. *Chem. Phys. Lett.* **1983**, *99*, 189.
(35) Bergund, B.; Vaughan, R. W. *J. Chem. Phys.* **1980**, *73*, 2037.

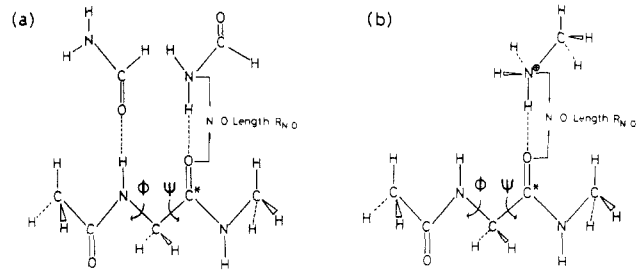

Figure 4. Molecular structure of *N*-acetyl-*N'*-methylglycine amide: (a) model A (taking the 1-type hydrogen bond with two formamide molecules) and (b) model B (taking the 2-type hydrogen bond with a protonated methylamine molecule). The calculation was made for the carbon marked by asterisks.

On the other hand, ^{13}C chemical shifts of the Gly CO are linearly displaced to upperfield with decreasing $R_{N\cdots O}$ in the 2-type hydrogen bond. The direction of the chemical shift change is opposite to that in the 1-type. Such a considerable difference between the two types of hydrogen bonds should be responsible for the electronic structure of the groups participating in the hydrogen bond. Detailed discussion about the electronic structure drawn on the basis of quantum chemical calculation will be given in the following section. A similar phenomenon was also reported for the hydrogen bond effect on nitrogen chemical shift that the direction and magnitude of the chemical shift change depend critically on the electronic environment around nucleus.[36]

As is seen in Figure 3a, the plots are slightly scattered from the dotted straight line. Such a scatter may come from the conformational effect of the skeletal bonds and the experimental errors for the determination of the hydrogen bond length. In spite of the dispersity in C=O···N angles, the 2-type hydrogen bond gave a clear linearity between the ^{13}C chemical shift and $R_{N\cdots O}$ compared with the 1-type. This can be attributed to the fact that the distribution of distortion angles ψ about the glycyl residue C_α–CO bond in the 2-type is much less than that in the 1-type. The direction effect of the hydrogen bond is thought to be small in the 2-type.

^{13}C Shielding Constant Calculation. Figures 5a–d and 6a–d show the calculated isotropic shielding constants (σ_{iso}) and their paramagnetic terms of tensor components (σ_{11}, σ_{22}, and σ_{33}) of Gly CO using the model compounds A and B (Figure 4, a and b) which correspond to the 1-type and 2-type hydrogen bonds, respectively. Calculated values are all expressed in parts per million (ppm) with an opposite sign to that of Table I. Note that the negative sign for the calculated shielding constant denotes deshielding, in contrast to the positive sign of the experimental chemical shift values. A shielding constant or tensor component is usually represented as a sum of the diamagnetic and the paramagnetic terms. However, the behavior of the shielding tensor can be explained by the paramagnetic term, since the diamagnetic term is isotropic.

Figure 5a shows the $R_{N\cdots O}$ dependence of the calculated isotropic ^{13}C shielding constant (σ_{iso}) of Gly CO in the 1-type hydrogen bond. In the region that $R_{N\cdots O}$ is larger than 2.6 Å, σ_{iso} values indicate no significant $R_{N\cdots O}$ dependence in both form I and form II. This means that there exists no hydrogen bond effect at $R_{N\cdots O}$ > 2.6 Å. As shown in Figure 5a, there is significant difference in σ_{iso} between form I and form II in this region. This may come from the conformation effect (conformation change) in going from form I to form II. On the other hand, in the region that $R_{N\cdots O}$ is shorter than 2.6 Å, σ_{iso} values largely depend on the hydrogen bond length $R_{N\cdots O}$, that is, the hydrogen bond effect is predominant. Therefore, the experimental data that the ^{13}C chemical shift values largely depend on $R_{N\cdots O}$ should be compared with the calculated results at $R_{N\cdots O}$ < 2.6 Å.

Here, we must be concerned with the critical $R_{N\cdots O}$ value being 2.6 Å. It seems that this value of 2.6 Å is somewhat short compared with the experimental data as shown in Figure 3. As the

(36) Webb, G. A.; Witanowski, M. *Proc. Indian Acad. Sci.* **1985**, *94*, 241.

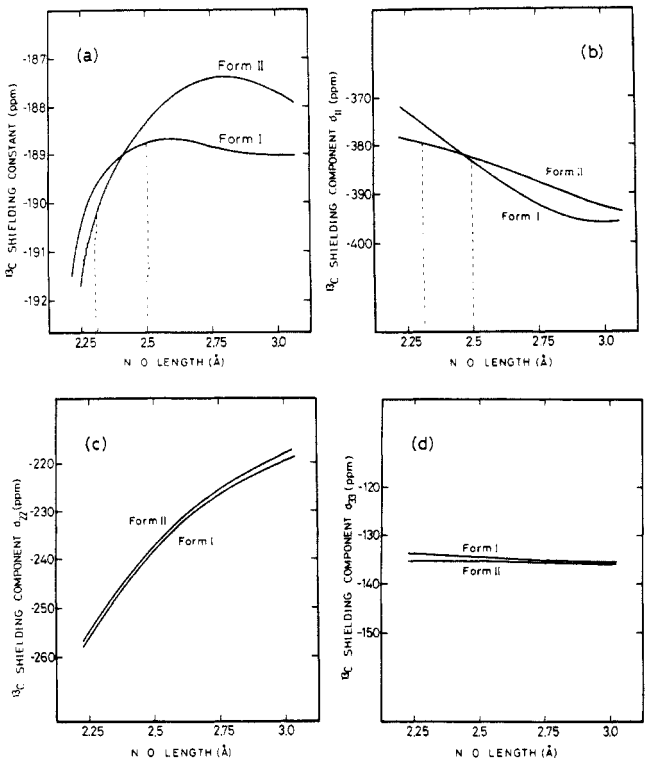

Figure 5. Variation of the calculated ^{13}C shielding constant and its tensor components with the N···O hydrogen bond length ($R_{N\cdots O}$) for the 1-type hydrogen bond: (a) isotropic shielding constant and (b) σ_{11}, (c) σ_{22}, and (d) σ_{33}.

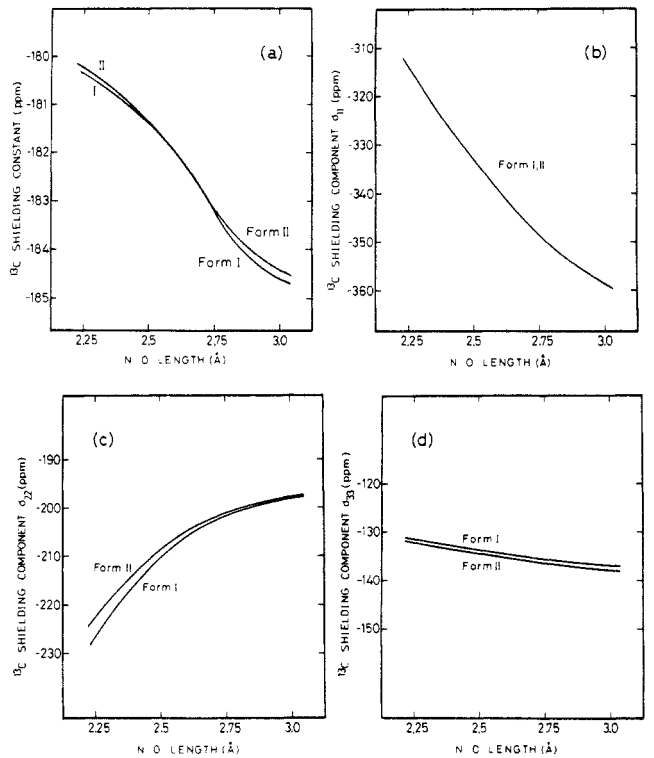

Figure 6. Variation of the calculated ^{13}C shielding constant and its tensor components with the N···O hydrogen bond length ($R_{N\cdots O}$) for the 2-type hydroge bond: (a) isotropic shielding constant and (b) σ_{11}, (c) σ_{22}, and (d) σ_{33}.

adopted semiempirical INDO MO approximation neglects some two-center electron integrals, the intermolecular interactions are considered to be reproduced reasonably in the short $R_{N\cdots O}$ region.[37] The variation of the total energy also supports this view as shown

(37) Morokuma, K. *Chem. Phys. Lett.* **1971**, *19*, 129.

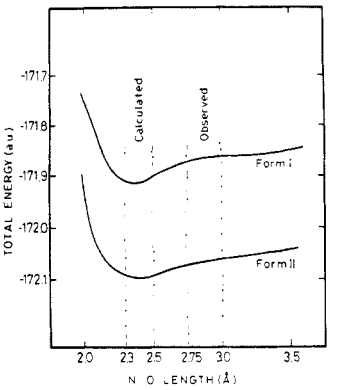

Figure 7. Variation of the calculated total energy for the 1-type hydrogen bond with model A.

in Figure 7, where the total energy minimum appears around the $R_{N\cdots O}$ value of 2.3–2.5 Å. Taking into consideration that the hydrogen bond length in a stable conformation is longer by 0.22 Å for $(Gly)_n$ I than for $(Gly)_n$ II,[2-4] the ^{13}C shielding constant at the $R_{N\cdots O}$ of 2.3 and 2.5 Å, as shown by the dotted line, should be taken for form II and form I, respectively. As a result, we obtain an appropriate σ_{iso} value for form II resonated at about 1.5 ppm downfield relative to form I. This reproduces the experimental result qualitatively. Although σ_{iso} shows a slightly complicated change with $R_{N\cdots O}$, each shielding component changes rather monotonously. As shown in Figure 5b–d, the particular change of σ_{iso} arises from the fact that σ_{11} increases with decreasing $R_{N\cdots O}$, while σ_{22} decreases with a comparable degree of change for σ_{11}. The difference of σ_{iso} between form I and form II at the $R_{N\cdots O} > 2.6$ Å region is due to the difference of σ_{11} component. This indicates that the above-mentioned conformation effect on σ_{iso} can be contributed by σ_{11}. However, the experimental finding that the σ_{11} is almost independent of conformational change, as reported previously,[1] is approximately reproduced in the shorter $R_{N\cdots O}$ region with regard for the difference of hydrogen bond length. On the other hand, the hydrogen bond effect is evident in the σ_{22} component, which is the dominant factor for the downfield shift in the shorter $R_{N\cdots O}$ region. Accordingly, it can be said that the σ_{11} component and the σ_{22} component reflect relatively the conformation effect and the hydrogen effect, respectively, in the 1-type. The calculated σ_{33} component is not sensitive to the changes of $R_{N\cdots O}$, while the observed σ_{33} component shows a relatively large displacement by changes of the $R_{N\cdots O}$ as reported previously.[1] If one judges from the large experimental error which arises from the overlapping of the C_α signal on the region of σ_{33} of the powder spectrum, it can be said that the σ_{33} component may reflect neither the conformation effect nor the hydrogen bond effect.

As shown in Figure 6a, the variation of σ_{iso} in the 2-type hydrogen bond gives a satisfactory coincidence with the experimental result. The magnitude of change for σ_{11} is much larger than that for σ_{22} and σ_{33}, and σ_{11} changes monotonically to upperfield with decreasing $R_{N\cdots O}$. It is entirely a dominant factor in determining the hydrogen bond dependence of the 2-type. Although the σ_{22} component represents the contribution of deshielding in the same manner as in the 1-type, this component does not contribute to the whole change of σ_{iso}. The hydrogen bond effect which appears in the σ_{11} component dominates the relative ^{13}C chemical shift of Gly CO in the 2-type, even in the $R_{N\cdots O} > 2.6$ Å region where the conformation effect is larger than the hydrogen bond effect in the 1-type. From the result of calculations, the origin of the difference in the experimental results between two types of hydrogen bonds is explicitly accounted for in terms of the σ_{11} component.

Figure 8a shows the directions of the principal axes of Gly CO ^{13}C chemical shift tensor components determined by the NMR study of [1-^{13}C]glycyl[^{15}N]glycine·HCl·H_2O single crystal,[38] and

(38) Stark, R. E.; Jelinski, L. W.; Rubin, D. J.; Torchia, D. A.; Griffin, R. G. *J. Magn. Reson.* **1983**, *55*, 266.

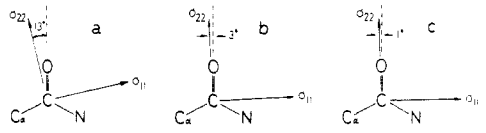

Figure 8. Orientation of the principal axes of the observed and calculated ^{13}C chemical shift tensors of glycyl residue carbonyl carbon in (a) glycylglycine·HCl·H_2O,[38] (b) model A (1-type hydrogen bond), and (c) model B (2-type hydrogen bond), respectively. The direction of σ_{33} (not shown here) is perpendicular to the directions of σ_{11} and σ_{22}.

parts b and c of Figure 8 show those determined by theoretical calculations performed in this study. The conformation of the model compounds indicated here is $(Gly)_n$ I and the $R_{N\cdots O}$ is 2.5 Å It is shown that a good agreement was obtained between the experimental and theoretical results. The σ_{22} component lies approximately along the amide CO bond, and the σ_{11} is in the amide sp^2 plane and lies along the direction normal to the C=O bond. The σ_{33} component is aligned in the direction perpendicular to the amide sp^2 plane. Kempf et al.[39] have pointed out that σ_{11} and σ_{22} components are dominated by singlet–singlet $\sigma-\pi^*$ and $n-\pi^*$ excitations, respectively. From a comparison of the behavior of the calculated σ_{11} and σ_{22} components between the two types of hydrogen bond, the nature of the proton-donating nitrogen atom is suggested to be very influencial to the electronic configuration of the σ bond near the carbonyl group, but it does not change the property of the nonbonding orbital located on the carbonyl oxygen. The σ_{22} component indicates a similar variation between the 1-type and 2-type hydrogen bonds, but σ_{11} show a considerable difference in the two types.

In the FPT–INDO calculation, since a shielding constant is expressed as a gradient of density matrix elements against the magnetic field,[13] the calculated shielding constant cannot be divided into contributions from certain one-electron excitations. However, such an effective contribution from a particular excitation can be attributed to the specific shielding components. Therefore, we can differentiate the hydrogen bond and conformational effect by elucidating the changes of each ^{13}C shielding component as described above.

The Conformational Dependence of the Gly CO Chemical Shift. In order to give a theoretical background to the conformation dependence of the ^{13}C chemical shift, Tonelli[40] attempted to explain the behavior of the chemical shift of polypeptides in terms of the empirical rule of the "gauche γ-effect". It has been revealed that this rule is very useful to interpret the ^{13}C chemical shifts of paraffinic hydrocarbons.[41] However, this attempt cannot be applied for elucidating the chemical shift behavior of C_α carbons of peptides. As pointed out by Saitô,[42] an argument of chemical shift displacement in terms of the gauche γ-effect can apply only to carbonyl and C_β carbons, not to the C_α carbon, because C_α carbons are located via trans (or rarely cis) arrangement across the amide bond from each other. Nevertheless, chemical shifts of the C_α carbon vary appreciably with a conformational change except for the case of polyglycine.[43-49] In addition, the chemical shift of the carbonyl carbon is thought to be characterized by the torsion angle ϕ and to be displaced upfield by several ppm when the angl ψ takes the value of about 60°. However, the carbonyl carbons of α-helical polypeptides are resonated downfield by 4–7 ppm relative to that for β-sheet forms.[43-49] Similarly, the Gly CO chemical shift of $(Gly)_n$ II is resonated downfield by 3.5 ppm from that for $(Gly)_n$ I.[1] It is noted that the ϕ values of the α-helical and 3_1-helical form of −58°[50] and −78°,[2] respectively, are in the allowable angle for the gauche conformation, while that of the β-sheet form is about −150°,[4] which is clearly different from the gauche angle.

As was mentioned above, $(Gly)_n$ II forms the shorter intermolecular hydrogen bond compared with $(Gly)_n$ I, and the α-helix form is generally stabilized by the strong intramolecular hydrogen bond. Apparently, the hydrogen bond plays an important role in determining the ^{13}C chemical shift of carbonyl carbons. Further, Pease et al.[51] reported the solid-state ^{13}C CP–MAS spectrum of a cyclic peptide, $(Gly\text{-}Phe\text{-}Gly)_2$, where a carbonyl carbon signal appears at the upfield region compared with that of the solution-state NMR. It was found that this molecule takes a symmetric form stabilized by two intramolecular hydrogen bonds in the solution state,[52] but this symmetry is lost in the crystalline state accompanying a cleavage of one of the two intramolecular hydrogen bonds.[53] The new signal appearing in the solid state could arise from the breakdown of one of the two hydrogen bonds which occurs by crystallization, because the angles of ϕ which are thought to affect to the chemical shifts of both Gly COs in the solid state are almost identical. On the other hand, Saitô et al.[49] reported that the Gly CO peaks of $(Pro\text{-}Gly\text{-}Pro)_n$ and $(Pro\text{-}Ala\text{-}Gly)_n$ taking collagen-like triple helices are displaced upfield by 5.1 and 4.1 ppm, respectively, compared with that of $(Gly)_n$ II. It is noted that there is no appreciable conformational difference between the triple helix and 3_1-helical $(Gly)_n$s. Gly CO in the triple helix does not participate in the hydrogen bond, while a strong hydrogen bond is formed in $(Gly)_n$ II. They show that the hydrogen bond causes the downfield shift in $(Gly)_n$ II. This coincides with the previous results obtained by the tight-binding MO calculation for $(Gly)_n$ I and II which takes into account the hydrogen bond between the interchains.[54]

As mentioned above, the quantum chemical calculation shows that the hydrogen bond effect on the chemical shift is dominant in the vicinity of the hydrogen bond length at $R_{N\cdots O} < 2.6$ Å, but at $R_{N\cdots O} > 2.6$ Å, the conformation effect becomes dominant as shown in Figure 5 because of the rapid reduction of the hydrogen bond strength owing to the increase of the hydrogen bond length. For polypeptides with no hydrogen bonds such as the above-mentioned $(Pro\text{-}Gly\text{-}Pro)_n$ and $(Pro\text{-}Ala\text{-}Gly)_n$, the chemical shift difference of 1 ppm between Gly COs of the two polypeptides is attributed only to their conformational change.

It can be said, therefore, that the quantum chemical calculation can separate successfully the conformational effect and the hydrogen bond effect on the chemical shift of Gly CO of peptides, the former being dominant in the region of long hydrogen bond length (or in no hydrogen bond) and the latter in the region of short hydrogen bond length. In other words, the Gly CO chemical shift in the solid state can be interpreted in terms of a change in electronic structure caused by the formation of hydrogen bond as well as conformational change.

Finally we can conclude as follows. The observed ^{13}C chemical shift in the amide type hydrogen bond moves linearly downfield with a decrease of the hydrogen bond length. This could be justified by quantum chemical calculation. These results may be applicable to the biopolymer field as a means for obtaining in-

(39) Kempf, J.; Spiess, H. W.; Haeberlen, U.; Zimmermann, H. *Chem. Phys.* **1974**, *4*, 269.
(40) (a) Tonelli, A. E. *J. Am. Chem. Soc.* **1980**, *102*, 7635. (b) Tonelli, A. E. *Biopolymers* **1984**, *23*, 819.
(41) Grant, D. M.; Paul, E. G. *J. Am. Chem. Soc.* **1964**, *86*, 2984.
(42) Saitô, H. *Magn. Reson. Chem.* **1986**, *24*, 835.
(43) Taki, T.; Yamashita, S.; Satoh, M.; Shibata, A.; Yamashita, T.; Tabeta, R.; Saitô, H. *Chem. Lett.* **1981**, 1803.
(44) Saitô, H.; Tabeta, R.; Shoji, A.; Ozaki, T.; Ando, I. *Macromolecules* **1983**, *16*, 1050.
(45) Saitô, H.; Tabeta, R.; Ando, I.; Ozaki, T.; Shoji, A. *Chem. Lett.* **1983**, 1437.
(46) Saitô, H.; Iwanaga, Y.; Tabeta, R.; Asakura, T. *Chem. Lett.* **1983**, 427.
(47) Saitô, H.; Tabeta, R.; Asakura, T.; Iwanaga, Y.; Shoji, A.; Ozaki, T.; Ando, I. *Macromolecules* **1984**, *17*, 1405.
(48) Shoji, A.; Ozaki, T.; Saitô, H.; Tabeta, R.; Ando, I. *Macromolecules* **1984**, *17*, 1472.
(49) Saitô, H.; Tabeta, R.; Shoji, A.; Ozaki, T.; Ando, I.; Miyata, T. *Biopolymers* **1984**, *23*, 2279.
(50) Ramachandran, G. N.; Sasisekharan, V. In *Advances in Protein Chemistry*; Academic: New York, 1968.
(51) Pease, L. G.; Frey, M. H.; Opella, S. J. *J. Am. Chem. Soc.* **1981**, *103*, 467.
(52) Pease, L. G.; Deber, C. M.; Blout, E. R. *J. Am. Chem. Soc.* **1973**, *95*, 258.
(53) Kostansek, E. C.; Thiessen, W. E.; Schomburg, D.; Lipscomb, W. N. *J. Am. Chem. Soc.* **1979**, *101*, 5811.
(54) Yamanobe, T.; Ando, I.; Saitô, H.; Tabeta, R.; Shoji, A.; Ozaki, T. *Bull. Chem. Soc. Jpn.* **1985**, *58*, 23.

formation about the hydrogen bond length or hydrogen bond strength in the solid state.

Registry No. H-Gly-Gly-Val-OH, 20274-89-9; ClAc-Gly-Gly-OH, 15474-96-1; H-Pro-Gly-Gly-OH, 7561-25-3; H-Ala-Gly-Gly-OH, 3146-40-5; H-Gly-Gly-OH, 556-50-3; H-Gly-Phe-Gly-OH, 14656-09-8; H-Gly-DL-Thr-OH, 27174-15-8; H-Gly-Thr-OH, 7093-70-1; H-Val-Gly-Gly-OH, 21835-35-8; H-Sar-Gly-Gly-OH, 18479-98-6; H-Gly-Gly-OH·HNO_3, 50998-12-4; H-DL-Leu-Gly-Gly-OH, 4337-37-5; H-Gly-DL-Phe-OH, 721-66-4; H-Gly-Phe-OH·HCl, 78410-67-0; H-Gly-Phe-OH·TsOH, 40301-89-1; H-Gly-OH, 56-40-6; glycine homopolymer, 25718-94-9; polyglycine, SRU, 25734-27-4.

Low-Temperature ^{13}C Magnetic Resonance. 8. Chemical Shielding Anisotropy of Olefinic Carbons[1a]

Anita M. Orendt, Julio C. Facelli, Alvin J. Beeler, Karl Reuter, W. J. Horton, Peter Cutts, David M. Grant,* and Josef Michl*[1b]

Contribution from the Department of Chemistry, University of Utah, Salt Lake City, Utah 84112. *Received August 14, 1987*

Abstract: The principal values of the ^{13}C NMR shielding tensor were measured at cryogenic temperatures for a series of olefinic carbons, including methyl-substituted ethylenes, 1-methyl- and 1,2-dimethylcycloalkenes, methylenecycloalkanes, and bicyclo[*n.m.*0]alkenes. Information on the orientation of the principal axes was obtained from ab initio calculations of the chemical shielding tensors using the IGLO (individual gauge for localized orbitals) method. The results for several compounds with unusual principal values of the shielding tensor were analyzed in terms of the bond contributions in the principal axis system.

Over the last several years the combination of low-temperature ^{13}C NMR spectroscopy with the quantum mechanical calculation of the chemical shielding tensor has been shown to be very valuable in the interpretation of chemical shielding data in small organic molecules.[2] Studies on carbon atoms in a wide range of bonding situations have been completed, including methyl groups,[3] methine carbons,[4] and methylene carbons.[5] Other studies have looked at carbons in linear molecules[6] and in the series cyclopropane, bicyclo[1.1.0]butane, and [1.1.1]propellane.[7] The calculations were used to determine the orientation of the principal axis system of the chemical shielding tensor in the molecular frame, information that is not determined experimentally from natural abundance powder samples.

Previously the experimental chemical shielding values for the cycloalkenes from cyclopropene to cyclooctene, ethylene, *cis*-2-butene, and *trans*-2-butene were reported.[8] For the sake of completeness these experimental results are also included here along with their calculated shielding tensors. A previous experiment on ethylene-*1,2*-$^{13}C_2$[9] provided the orientation of the principal axis system in the molecular frame. The findings were that the downfield component, σ_{11}, was perpendicular to the double bond and lay in the plane of the molecule, σ_{22} was along the double bond, and σ_{33} was perpendicular to the double bond and to the plane of the molecule. Similar orientations have been found in several single-crystal studies,[10,11] and in another dipolar study[12] on more complicated alkene derivatives. Early theoretical studies have also shown the same results for the orientation of the shielding tensors.[13-16]

In this paper, the experimental principal values of the shielding tensor as well as the calculated results are presented for a wide range of olefinic carbons. The types of olefinic carbons that are studied can be divided into five groups: methyl-substituted ethylenes, cycloalkenes, 1-methyl- and 1,2-dimethylcycloalkenes, methylenecycloalkanes, and bicyclo[*n.m.*0]alkenes. The structures of the compounds studied are shown in Figure 1.

Experimental and Computational Methods

Materials. Commercial samples of tetramethylethylene, methylenecyclobutane, methylenecyclopentane, propene, 1-methylcyclopentene, and isobutene were used without any further purification. A sample of 1,2-dimethylcyclobutene was provided by Professor D. Aue (University of California at Santa Barbara). The precursor for the synthesis of bicyclo[2.2.0]hex-1(4)-ene as well as a sample of bicyclo[3.2.0]hept-1(4)-ene was provided by Professor K. B. Wiberg (Yale University). Drs. P. J. Okarma and J. J. Caringi (Yale University) provided a sample of bicyclo[3.3.0]oct-1(5)-ene.

The remaining compounds were synthesized according to published literature procedures: methylenecyclopropane,[17] 1,2-bismethylenecyclobutane,[18] 1,2-dimethylcyclohexene,[19] bicyclo[3.2.0]hept-1(5)-ene,[20] bi-

(1) (a) For part 7 in this series, see ref 3. (b) Present address: Department of Chemistry, University of Texas at Austin, Austin, Texas 78712-1167.
(2) Facelli, J. C.; Grant, D. M.; Michl, *J. Acc. Chem. Res.* **1987**, *20*, 152.
(3) Solum, M. S.; Facelli, J. C.; Michl, J.; Grant, D. M. *J. Am. Chem. Soc.* **1986**, *108*, 6464.
(4) Facelli, J. C.; Orendt, A. M.; Solum, M. S.; Depke, G.; Grant, D. M.; Michl, J. *J. Am. Chem. Soc.*, **1986**, *108*, 4268.
(5) Facelli, J. C.; Orendt, A. M.; Beeler, A. J.; Solum, M. S.; Depke, G.; Malsch, K. D.; Downing, J. W.; Murthy, P. S.; Grant, D. M.; Michl, J. *J. Am. Chem. Soc.* **1985**, *107*, 6749.
(6) Beeler, A. J.; Orendt, A. M.; Grant, D. M.; Cutts, P. W.; Michl, J.; Zilm, K. W.; Downing, J. W.; Facelli, J. C.; Schindler, M.; Kutzelnigg, W. *J. Am. Chem. Soc.* **1984**, *106*, 7672.
(7) Orendt, A. M.; Facelli, J. C.; Grant, D. M.; Michl, J.; Walker, F. H.; Dailey, W. P.; Waddell, S. T.; Wiberg, K. B.; Schindler, M.; Kutzelnigg, W. *Theor. Chim. Acta* **1985**, *68*, 421.
(8) Zilm, K. W.; Conlin, R. T.; Grant, D. M.; Michl, J. *J. Am. Chem. Soc.* **1980**, *102*, 6672.
(9) Zilm, K. W.; Grant, D. M. *J. Am. Chem. Soc.* **1981**, *103*, 2913.
(10) Wolff, E. K.; Griffin, R. G.; Waugh, J. S. *J. Chem. Phys.* **1977**, *67*, 2387.
(11) Igner, D.; Fiat, D. *J. Magn. Reson.* **1982**, *46*, 233.
(12) Manenschijn, A.; Duijvestijn, M. J.; Smidt, J.; Wind, R. A.; Yannoni, C. S.; Clarke, T. C. *Chem. Phys. Lett.* **1984**, *112*, 99.
(13) Ditchfield, R.; Ellis, P. D. In *Topics in ^{13}C NMR Spectroscopy*; Wiley: New York, 1974; Vol. 1.
(14) Ditchfield, R.; Miller, D. P.; Pople, J. A. *J. Chem. Phys.* **1971**, *54*, 4186.
(15) Strong, A. B.; Ikenberry, D.; Grant, D. M. *J. Magn. Reson.* **1973**, *9*, 145; errata: **1976**, *21*, 157.
(16) Ebraheem, K. A. K.; Webb, G. A. In *Progress in NMR Spectroscopy*; Pergamon Press: Oxford, 1977; Vol. 11.
(17) Salaun, J. R.; Champion, J.; Conia, J. M. *Org. Synth.* **1977**, *57*, 36.
(18) Borden, W. T.; Reich, I. L.; Sharpe, L. A.; Weinberg, R. B.; Reich, H. J. *J. Org. Chem.* **1975**, *40*, 2438.

0002-7863/88/1510-3386$01.50/0